

## Primakoff Production of the $B^+(1235)$ Meson

B. Collick, S. Heppelmann, T. Joyce, Y. Makdisi,<sup>(a)</sup> M. L. Marshak, E. A. Peterson, and K. Ruddick  
*University of Minnesota, Minneapolis, Minnesota 55455*

and

D. Berg,<sup>(b)</sup> C. Chandlee, S. Cihangir,<sup>(c)</sup> T. Ferbel, J. Huston, T. Jensen,<sup>(d)</sup> F. Lobkowicz,  
 T. Ohshima,<sup>(e)</sup> P. Slattery, P. Thompson,<sup>(a)</sup> and M. Zielinski<sup>(f)</sup>  
*University of Rochester, Rochester, New York 14627*

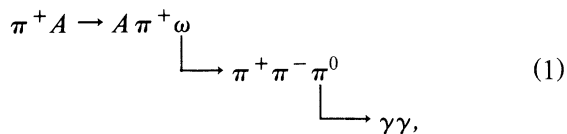
and

A. Jonckheere and C. A. Nelson, Jr.  
*Fermi National Accelerator Laboratory, Batavia, Illinois 60510*  
 (Received 30 July 1984)

We have measured the coherent nuclear production of  $\pi^+\omega$  systems at 202.5 GeV. This final state is dominated by the  $B^+(1235)$  meson with a measured mass and full width of  $1.271 \pm 0.011$  GeV and  $0.232 \pm 0.029$  GeV, respectively. A radiative width of  $230 \pm 60$  keV was extracted for the process  $B^+(1235) \rightarrow \pi^+\gamma$ .

PACS numbers: 13.40.-f, 13.40.Hq, 13.85.Hd, 14.40.Cs

In an experiment at the Fermi National Accelerator Laboratory, we have studied the properties of the  $B^+(1235)$  meson produced via the coherent reaction



using a 202.5-GeV pion beam incident on Cu and Pb targets. At these energies, the purely electromagnetic Primakoff process<sup>1</sup> is expected to dominate coherent production at very small values of  $t$ , the four-momentum transfer squared. These measurements were part of a comprehensive experiment<sup>2</sup> designed to determine the electromagnetic couplings of spin-1 and spin-2 mesons to pseudo-scalar mesons. Such data provide stringent tests of specific quark-model calculations of spin transition rates.<sup>3</sup> In addition, electromagnetic production provides a particularly clean regime for examining the properties of a particular elementary particle.

The experimental apparatus has been described previously in detail.<sup>2</sup> Its salient features included a secondary beam equipped with Cherenkov counters and trajectory-defining proportional chambers, a drift- and proportional-chamber forward magnetic spectrometer, and a finely segmented liquid-argon calorimeter. This latter device was located downstream of the magnetic spectrometer.

Beam  $K^+$  decays in flight to  $\pi^+\pi^0$ ,  $\pi^+\pi^+\pi^-$ , and  $e^+\pi^0\nu$  were recorded simultaneously with the coherent scattering data. These decays were used to determine the resolution of the spectrometer, veri-

fy the reliability of the Monte Carlo model of the apparatus, and check the absolute normalization of the measured cross sections.

The data reported here were derived from one of several simultaneous triggers used for this apparatus. The particular trigger used here required a pulse height indicating three minimum-ionizing particles in a scintillation counter, located just downstream of the target, two to four charged tracks in the spectrometer's proportional chambers, and no hits in the veto scintillation counters. These latter devices were designed to detect noncoherent reactions. In total,  $7.5 \times 10^6$  events were recorded and analyzed to obtain this data sample.

The following requirements were imposed on the data to isolate the final state identified in Reaction (1): (a) identification of the incident particle as a pion; (b) a final state consisting of two photons and three charged tracks (two positive, one negative); (c) a reconstructed interaction point located in the target; (d) reconstruction of the two  $\gamma$ 's as a  $\pi^0$  within the experimental resolution; and (e) no measurable energy loss between the initial and final state.

Figure 1(a) shows the  $\pi^+\pi^-\pi^0$  effective-mass spectrum for the  $4\pi$  events selected by means of these cuts. The plot has two entries per event, representing the two possible choices for the  $\pi^+$ . Clear  $\eta$  and  $\omega$  signals are seen. The  $\eta$ 's are primarily from  $A_2$  decays which have been analyzed previously<sup>4</sup>; they can be considerably reduced by a cut on  $|t| < 0.005$  (GeV/c)<sup>2</sup>. The procedure of plotting two entries per event overemphasizes the back-

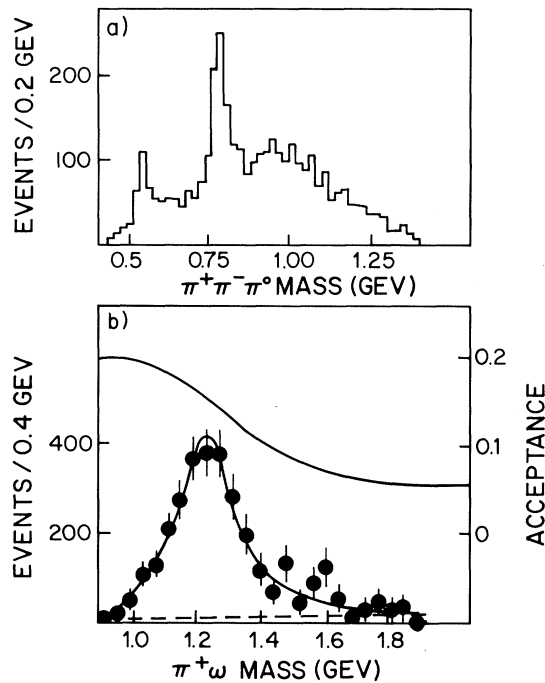


FIG. 1. (a) The  $\pi^+\pi^-\pi^0$  mass for events selected according to the cuts listed in the text. There are two mass combinations plotted for each event. (b) The  $\pi^+\omega$  mass distribution (acceptance corrected) for events selected from the plot above, for both Cu and Pb targets. The experimental acceptance is shown by the line above the data. The dashed curve indicates the amount of background required by the fit.

ground under the  $\eta$  and  $\omega$  peaks. The actual background under the  $\omega$  peak was estimated as  $\leq 20\%$  from a study of events near to but outside the peak.

Figure 1(b) shows the  $\pi^+\omega$  invariant-mass distribution for events with a  $3\pi$  mass in the  $\omega$  region (0.74–0.82 GeV) and with four-momentum transfer  $-t < 0.005$  (GeV/c)<sup>2</sup>. Excluded from the plot are events with either  $3\pi$  mass combination in the  $\eta$  region. These data have been corrected with use of the calculated experimental acceptance shown in the figure. The  $\pi^+\omega$  mass distribution is clearly dominated by a single peak.

The superimposed curve is a fit to the mass spectrum by a relativistic  $p$ -wave Breit-Wigner resonance modified by the coherent production process,<sup>2</sup> plus polynomial terms for the background. (The polynomial form for the background yielded a more probable fit than other forms, including a polynomial plus a Gaussian with a peak under the resonance.) The background as shown, integrated from 1.0 to 1.8 GeV, comprises 13% of the signal, in reasonable agreement with the  $\leq 20\%$  value estimated in connection with Fig. 1(a). The fit yields

a mass of  $1.271 \pm 0.011$  GeV and a width of  $0.232 \pm 0.029$  GeV. The mass is shifted from the apparent centrum of the peak in Fig. 1(b) by the approximately  $1/m^3$  dependence of the Primakoff cross section. The chi-squared for the fit is 0.9/DOF. The most probable identification of this peak is with the  $B^+(1235)$  resonance.

The mass and width reported here are larger than the standard values for the  $B^+$  meson.<sup>5</sup> Previous data were obtained in strong-interaction processes and may have been subject to substantial interference and background effects that are not as severe in this experiment. Measurements of masses and widths of the  $\rho^-$ ,  $K^{*+}$ ,  $K^{*+}(1420)$ , and  $A_2^+$  mesons, previously reported by this collaboration,<sup>6</sup> have all agreed with standard values, which argues against a systematic energy-scale error in this experiment. (These other states were observed with a considerably smaller width than the  $B$ , so that the  $1/m^3$  production dependence had a much smaller effect on the resonance peak.) A recent photoproduction experiment<sup>7</sup> has observed a  $B$ -meson width of 0.230 GeV, consistent with the measurement reported here. However, the  $B$ -meson mass in those data was 1.215 GeV, which is significantly lower than our value. We currently do not know of any explanation for these discrepancies, other than the general observation that backgrounds and kinematic factors can cause masses and widths to appear to vary for different production processes.

We have investigated the angular distributions of the sequential decays  $B^+ \rightarrow \pi^+\omega$ ,  $\omega \rightarrow \pi^+\pi^-\pi^0$ , and the  $t$  distribution for  $B$ -meson production. The events used for these analyses were required to have a  $\pi^+\omega$  mass between 1.0 and 1.4 GeV. In this mass region, the non- $B$  background from Fig. 1(b) is  $\approx 6\%$ . The data used for these analyses were corrected for this background level.

The goal of the decay-angle analysis was to check the spin and parity of the observed peak to determine whether it was characterized by unnatural spin and parity, which would help confirm the identification of the resonance as the  $B$ . The amplitude for this sequential decay is<sup>8</sup>

$$M \propto \sum_{\lambda} F_{\lambda} D_{m\lambda}^{*j}(\Phi, \Theta, 0) D_{\lambda 0}^{*i}(\phi, \theta, 0), \quad (2)$$

where  $F_{\lambda}$  is the helicity amplitude of the  $\omega$  ( $\sum_{\lambda} |F_{\lambda}|^2 = 1$ ),  $\Phi$  and  $\Theta$  are the polar and azimuthal angles of the  $\omega$  in the  $B$  rest frame, and  $\phi$  and  $\theta$  are the polar and azimuthal angles of the normal to the  $\omega$  decay plane. In the  $B$  rest frame, the  $z$  axis is parallel to the momentum vector of the meson (helicity frame) and the  $y$  axis is normal to the production plane. The angles  $\phi$  and  $\theta$  are measured in

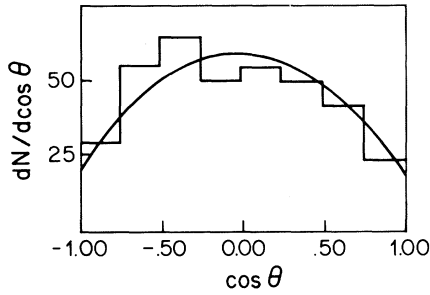


FIG. 2. The decay angular distribution defined in the text. The curve is a fit which is also described in the text.

the  $\omega$  rest frame with the  $z'$  axis defined parallel to the momentum vector of the  $\omega$  and  $\bar{y}' = \bar{z} \times \bar{z}'$ . In this experiment,  $\Phi$  was not well determined because the extremely small  $t$  resulted in a poor definition of the production plane. On the other hand,  $\Theta$  was well defined on an event-by-event basis, but variations in the experimental acceptance dominated the  $\cos\Theta$  distribution. Monte Carlo studies, however, indicate good resolution and a flat acceptance for  $\theta$  and  $\phi$ .

Parity conservation in the decay  $B \rightarrow \pi\omega$  requires that  $F_\lambda = \epsilon F_{-\lambda}$ , where  $\epsilon = -P(-1)^J$  with  $P$  representing the parity of the  $B$  meson.<sup>8</sup> The helicity amplitudes can be evaluated by study of the  $\cos\theta$  distribution given by<sup>8</sup>

$$\frac{d\sigma}{d\cos\theta} = \frac{3}{2}(|F_0|^2 \cos^2\theta + |F_1|^2 \sin^2\theta). \quad (3)$$

Figure 2 shows that the data are dominated by the second term. However, the value of  $|F_0|^2$  determined by a maximum-likelihood fit<sup>8</sup> is  $0.16 \pm 0.03$ , which is significantly nonzero and consistent with previous measurements.<sup>9</sup> This value for the  $F_0$  term indicates that the observed resonance must have unnatural spin and parity (i.e.,  $1^+, 2^-, 3^+, \dots$ ) which is consistent with the standard assignment<sup>8</sup> of the  $B^+(1235)$  meson ( $J^P=1^+$ ). Thus, the spin and parity analysis confirms the identification of the observed peak as the  $B^+(1235)$  meson.

The total coherent differential cross section for  $B$  production can be written as

$$d\sigma/dt = |T_c + e^{i\phi}T_s|^2, \quad (4)$$

where  $T_c$  is the electromagnetic production amplitude and  $T_s$  is the strong interaction amplitude.  $T_c$  is proportional to the radiative width  $\Gamma_\gamma(B^+ \rightarrow \pi^+\gamma)$  and is sharply peaked near  $t=0$ .  $T_s$  can be written in terms of  $C_s$ , which is the strength parameter for coherent strong production on a nu-

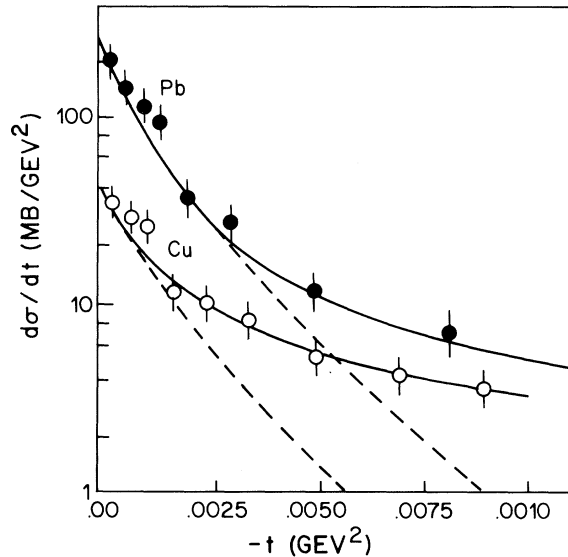


FIG. 3. The measured differential cross section for coherent production of the  $\pi^+\omega$  system from Cu and Pb targets. The solid line is a fit to the data; the dashed line is the contribution of only the electromagnetic amplitude to the cross section. The shape of the dashed curves was calculated with use of the equations of Ref. 1.

cleon. The detailed parametrizations of each of these scattering amplitudes can be found elsewhere.<sup>10</sup>

Figure 3 shows the differential cross sections measured in this experiment for the Pb and Cu targets. These cross sections were fitted by varying the parameters  $\Gamma_\gamma$ ,  $C_s$ , and the relative phase  $\phi$ . They have been corrected for the observed background. The latter two quantities were not well determined because of the dominance of the electromagnetic channel. The acceptable range for  $C_s$  varied from 1 to 4 mb/(GeV/c)<sup>4</sup>. The radiative width,  $\Gamma_\gamma$ , was determined to be 230 keV with a systematic error of 30 keV. (The systematic error is determined from the fitting process. This width value also assumes that the  $B$  decays hadronically only to  $\omega\pi$ .) This uncertainty, combined in quadrature with a 35-keV statistical error and a 15% normalization error, yielded a radiative width and error of  $230 \pm 60$  keV.

Our result agrees reasonably with predictions based on single-quark transitions and a vector-dominance model.<sup>3</sup> If we use the values for the mass, full width, and  $F_0$  measured in this experiment, the predicted radiative width is  $274 \pm 48$  keV. The previous world averages for these parameters yield a prediction of  $184 \pm 30$  keV.

In summary, we have measured the differential

cross section for coherent production of the  $\pi^+\omega$  final state at 200-GeV incident energy. These data demonstrate the dominance of the Primakoff effect on Cu and Pb targets for  $-t < 0.002$  (GeV/c)<sup>2</sup>. The Primakoff cross section itself is dominated by a single resonant state which we have identified through its mass, width, decay modes, and parity assignment as the  $B^+(1235)$ . We have determined new values for the mass and width of this state, which are less likely to be affected by background than previous strong-interaction measurements. The measured radiative width  $\Gamma_\gamma$  is consistent with quark-model predictions that also explain other radiative widths measured in this experiment.

This research was supported by the U. S. Department of Energy and the National Science Foundation.

---

<sup>(a)</sup>Presently at Brookhaven National Laboratory, Upton, N.Y. 11973

<sup>(b)</sup>Presently at Fermilab, Batavia, Ill. 60510.

<sup>(c)</sup>Presently at University of Illinois, Urbana, Ill. 61801.

<sup>(d)</sup>Presently at Ohio State University, Columbus, Ohio 43210.

<sup>(e)</sup>Presently at the Institute for Nuclear Study, University of Tokyo, Japan.

<sup>(f)</sup>Presently at Jagellonian University, Krakow, Poland.

<sup>1</sup>H. Primakoff, Phys. Rev. **81**, 899 (1951); A. Halprin, C. M. Anderson, and H. Primakoff, Phys. Rev. **152**, 1295 (1966); G. Berlad *et al.*, Ann. Phys. (N.Y.) **75**, 461 (1973); L. Stodolsky, Phys. Rev. **144**, 1145 (1966).

<sup>2</sup>T. Jensen *et al.*, Phys. Rev. D **27**, 26 (1983); C. Nelson *et al.*, Nucl. Instrum. Methods **216**, 381 (1983).

<sup>3</sup>J. Babcock and J. L. Rosner, Phys. Rev. D **14**, 1286 (1976); J. L. Rosner, Phys. Rev. D **23**, 1127 (1981), P. J. O'Donnell, Rev. Mod. Phys. **53**, 673 (1981).

<sup>4</sup>S. Cihangir, Ph.D. thesis, University of Rochester, 1981 (unpublished).

<sup>5</sup>C. G. Wohl *et al.* (Particle Data Group), Rev. Mod. Phys. **56**, S1 (1984).

<sup>6</sup>D. Berg *et al.*, Phys. Lett. **99B**, 119 (1981); C. Chandlee *et al.*, Phys. Rev. Lett. **51**, 168 (1983); S. Cihangir *et al.*, Phys. Lett. **117B**, 119 (1982); S. Cihangir *et al.*, Phys. Lett. **117B**, 123 (1982).

<sup>7</sup>M. Atkinson *et al.*, to be published.

<sup>8</sup>S. U. Chung, Phys. Rev. **138**, B1541 (1965), and CERN Report No. CERN 71-8 (1971); M. Afzal *et al.*, Nuovo Cimento **A15**, 61 (1973); S. U. Chung *et al.*, Phys. Rev. D **11**, 2426 (1975).

<sup>9</sup>V. Chaloupka *et al.*, Phys. Lett. **51B**, 407 (1974); U. Karshon *et al.*, Phys. Rev. D **10**, 3608 (1974); S. U. Chung *et al.*, Phys. Rev. D **11**, 2426 (1975); R. Gassaroli *et al.*, Nucl. Phys. **B126**, 382 (1977).

<sup>10</sup>G. Faldt, Nucl. Phys. **B43**, 591 (1972); C. Bemporad *et al.*, Nucl. Phys. **B51**, 1 (1973); see also Jensen *et al.*, Ref. 2.